Frequency domain quantum optimal control under multiple constraints

Chuan-Cun Shu,[1,2,*] Tak-San Ho,[1,†] Xi Xing,[1] and Herschel Rabitz[1,‡]
[1]*Department of Chemistry, Princeton University, Princeton, New Jersey 08544, USA*
[2]*School of Engineering and Information Technology, University of New South Wales at the Australian Defence Force Academy, Canberra ACT 2600, Australia*

(Received 15 January 2016; published 23 March 2016)

Optimal control of quantum systems with complex constrained external fields is one of the longstanding theoretical and numerical challenges at the frontier of quantum control research. Here, we present a theoretical method that can be utilized to optimize the control fields subject to multiple constraints while guaranteeing monotonic convergence towards desired physical objectives. This optimization method is formulated in the frequency domain in line with the current ultrafast pulse shaping technique, providing the possibility for performing quantum optimal control simulations and experiments in a unified fashion. For illustrations, this method is successfully employed to perform multiple constraint spectral-phase-only optimization for maximizing resonant multiphoton transitions with desired pulses.

DOI: 10.1103/PhysRevA.93.033417

I. INTRODUCTION

Controlling quantum mechanical systems with temporally shaped ultrafast laser pulses has drawn increasing interest driven by laboratory technological advances and a growing number of applications in quantum sciences and technologies [1–7]. The time-dependent electric field of a laser pulse can be written as

$$\mathcal{E}(t) = \mathrm{Re}\left[\int_0^\infty \boldsymbol{\epsilon}(\omega)\exp(-i\omega t)d\omega\right], \tag{1}$$

where the complex-valued spectral field $\boldsymbol{\epsilon}(\omega)$ can be defined by $\boldsymbol{\epsilon}(\omega) = A(\omega)\exp[i\phi(\omega)]$ in terms of the real-valued spectral amplitude $A(\omega) \geqslant 0$ and the real-valued spectral phase $\phi(\omega)$. Quantum optimal control theory (QOCT) has provided a powerful tool to explore optimal applied field shaping of quantum system dynamics, including the control of electrons in quantum dots [8], manipulation of quantum many-body dynamics [9], and construction of quantum entangling gates [10]. Many QOCT approaches have been developed to directly optimize the time domain control fields $\mathcal{E}(t)$ ignoring various types of constraints [11–17]. However, ultrafast pulse shaping techniques used to date in quantum optimal control experiments (QOCEs) [18–22] are based on the manipulation of the spectral field $\boldsymbol{\epsilon}(\omega)$ in the frequency domain [23,24], and thus experimentally optimized pulses naturally include various internal limitations (e.g., limited bandwidth, finite pixel resolution, etc.). Moreover, optimal control fields may be further required to comply with various external constraints (e.g., low peak intensity for avoiding sample damage, and short enough pulse length for combating decoherence). In this context, a general QOCT method capable of incorporating multiple constraints would be desirable in making theoretical studies closer to experimental realism. Due to various challenges involved in acquiring either monotonic convergence or general applicability of the algorithms [25], only recently have there been limited attempts to take strict limitations on the spectral amplitude of the optimized laser fields into account by modifying the time-domain QOCT methods [26–31].

In this work, we present a frequency domain quantum optimal control method that may be employed in simulations *as well as* experiments to search for optimal pulses subject to multiple internal limitations as well as external constraints while guaranteeing monotonic convergence towards desired physical objectives. Importantly, the method is derived without making any assumptions on the nature of the quantum system, ensuring its applicability to general ultrafast photophysical and photochemical processes. For illustrations, we employ this optimization method to perform multiple constraint spectral-phase-only optimization (SPOO) by fixing the spectral amplitude as one of internal limitations and imposing desired external constraints on the spectral phase. The SPOO has been widely employed in QOCEs for diverse applications [18–22], because this approach has the advantages of conserving the pulse energy while highlighting the effect of quantum coherence phenomena [32–34]. However, since previously proposed QOCT methods developed in the time domain are not straight forward to optimize the spectral phase, the implementation of SPOO in QOCT simulations was rare [33,35]. In particular, we examine how a nonlinear optical phenomenon of resonant multiphoton transition can be affected by shaping the spectral phase of a single control pulse.

II. GENERAL FORMULATION

To show the generality of the method, we consider an arbitrary physical objective J (i.e., the expectation value of any observable quantity). Like the time domain DMORPH optimization algorithm [36], a dummy variable $s \geqslant 0$ is employed to track the trajectory of the optimization of the spectral field $\boldsymbol{\epsilon}(\omega)$ with $\boldsymbol{\epsilon}(s,\omega)$. As s is increased, the change in the control objective can be written using the chain rule as

$$g_0(s) \equiv \frac{dJ}{ds} = \int_0^\infty \frac{\delta J}{\delta\boldsymbol{\epsilon}(s,\omega)}\frac{\partial\boldsymbol{\epsilon}(s,\omega)}{\partial s}d\omega \geqslant 0. \tag{2}$$

Without incorporating constraints on the field, maximizing J that requires $dJ/ds \geqslant 0$ can be assured by integrating the

*c.shu@adfa.edu.au
†tsho@princeton.edu
‡hrabitz@princeton.edu

following equation

$$\frac{\partial \epsilon(s,\omega)}{\partial s} = \left[\frac{\delta J}{\delta \epsilon(s,\omega)}\right]^*, \tag{3}$$

starting from an initial spectral field $\epsilon(0,\omega)$ at $s = 0$. Likewise, minimizing J that requires $dJ/ds \leqslant 0$ can be obtained by setting $\partial\epsilon(s,\omega)/\partial s = -[\delta J/\delta\epsilon(s,\omega)]^*$.

Equation (3) can be generalized to include a set of external constraints satisfying the equalities $h_\ell[\epsilon(s,\cdot)] = C_\ell$, $\ell = 1,\ldots,M$, to restrict the spectral field $\epsilon(s,\omega)$, resulting in M null-integral equalities

$$g_\ell(s) \equiv \frac{dh_\ell}{ds} = \int_0^\infty \frac{\delta h_\ell}{\delta\epsilon(s,\omega)}\frac{\partial\epsilon(s,\omega)}{\partial s}d\omega = 0 \tag{4}$$

indicating that $\partial\epsilon(s,\omega)/\partial s$ is orthogonal to all constraint gradients $\delta h_\ell/\delta\epsilon(s,\omega)$. The combined demands in Eqs. (2) and (4) can be simultaneously fulfilled by expressing $\partial\epsilon(s,\omega)/\partial s$ as

$$\frac{\partial\epsilon(s,\omega)}{\partial s} = g_0(s)\int_0^\infty S(\omega'-\omega)\sum_{\ell=0}^{M}[\Gamma^{-1}]_{0\ell}c_\ell^*(s,\omega')d\omega', \tag{5}$$

where the convolution function $S(\omega'-\omega)$ is additionally introduced as the filter to remove unwanted components of the spectral field, and Γ is an $(M+1)\times(M+1)$ symmetric matrix composed of the elements $\Gamma_{kk'} = \int_0^\infty c_k(s,\omega)\int_0^\infty S(\omega'-\omega)c_{k'}^*(s,\omega')d\omega' d\omega$ with coefficients

$$c_\ell(s,\omega) = \begin{cases} \frac{\delta J}{\delta\epsilon(s,\omega)}, & \ell = 0 \quad (6a)\\ \frac{\delta h_\ell}{\delta\epsilon(s,\omega)}, & \ell = 1,\ldots,M. \quad (6b)\end{cases}$$

The inverse of the matrix Γ is assumed to exist such that $\Gamma^{-1}\Gamma = 1$. In the case that Γ is ill conditioned (i.e., its condition number is large), efficient regularization procedures can be implemented to approximate the inverse matrix Γ^{-1} [37]. By inserting Eq. (5) into Eqs. (2) and (4) we can verify that

$$\begin{aligned} g_{\ell'}(s) &= g_0(s)\int_0^\infty c_{\ell'}(s,\omega)\int_0^\infty S(\omega'-\omega)\\ &\quad\times\sum_{\ell=0}^{M}[\Gamma^{-1}]_{0\ell}c_\ell^*(s,\omega')d\omega' d\omega\\ &= g_0(s)\sum_{\ell=0}^{M}[\Gamma^{-1}]_{0\ell}\Gamma_{\ell\ell'}\\ &= g_0(s)\delta_{0\ell'}, \quad \ell' = 0,1,\ldots,M, \end{aligned} \tag{7}$$

is always greater than ($\ell' = 0$) or equal ($\ell' \neq 0$) to zero, implying that both monotonic convergence and the imposed external constraints in Eqs. (2) and (4) are satisfied simultaneously.

Since the gradients $\delta h_\ell/\delta\epsilon(s,\omega)$ in Eq. (6) can be directly calculated, the key to utilizing the method in simulations as well as in experiments is to obtain $\delta J/\delta\epsilon(s,\omega)$ in Eq. (6a). In practice, we may separately calculate the gradients of J with respect to $A(s,\omega)$ and $\phi(s,\omega)$ based on the current pulse shaping technique, in which the spectral amplitude and phase can be separately manipulated with different modulators [23,24]. In experiments, the gradients $\delta J/\delta A(s,\omega)$ and $\delta J/\delta\phi(s,\omega)$ can be measured with stochastic sampling methods [38]. In simulations, we have $\delta J/\delta A(s,\omega) = \int_{-\infty}^{\infty}[\delta J/\delta\mathcal{E}(s,t)][\partial\mathcal{E}(s,t)/\partial A(s,\omega)]dt$ and $\delta J/\delta\phi(s,\omega) = \int_{-\infty}^{\infty}[\delta J/\delta\mathcal{E}(s,t)][\partial\mathcal{E}(s,t)/\partial\phi(s,\omega)]dt$, where $\partial\mathcal{E}(s,t)/\partial A(s,\omega) = \cos[\phi(s,\omega) - i\omega t]$ as well as $\partial\mathcal{E}(s,t)/\partial\phi(s,\omega) = -A(\omega)\sin[\phi(s,\omega) - i\omega t]$ can be derived from Eq. (1), and $\delta J/\delta\mathcal{E}(s,t)$ can be computed by solving the time evolution equations of quantum systems [28,36]. For a general N-level closed quantum system, the control objective J associated with an observable O at the final time $T/2$ can be defined by

$$J = \mathrm{Tr}\left[U\left(\frac{T}{2},-\frac{T}{2}\right)\rho_0 U^\dagger\left(\frac{T}{2},-\frac{T}{2}\right)O\right], \tag{8}$$

where ρ_0 is the density operator at the initial time $-T/2$. The evolution operator U of the quantum system interacting with control fields $\mathcal{E}(s,t)$ can be described by the time-dependent Schrödinger equation $\partial_t U(t,-T/2) = -i[H_0 - \mu\mathcal{E}(t)]U(t,-T/2)$ subject to the initial condition $U(-\frac{T}{2},-\frac{T}{2}) \equiv \mathbb{I}$, where H_0 is the field-free Hamiltonian, and μ the dipole moment operator. The gradient of J with respect to $\mathcal{E}(s,t)$ can thus be written as

$$\frac{\delta J}{\delta\mathcal{E}(s,t)} = -2\mathrm{Im}\left(\mathrm{Tr}\left\{\left[\rho_0, O\left(\frac{T}{2}\right)\right]\mu(t)\right\}\right), \tag{9}$$

with $\mu(t) = U^\dagger(t,-T/2)\mu U(t,-T/2)$ and $O(T/2) = U^\dagger(T/2,-T/2)OU(T/2,-T/2)$. Equation (5) can be solved (e.g., by using the Euler method) to update the spectral field from $\epsilon(s,\omega)$ to $\epsilon(s+ds,\omega)$ over the control variable s until the control objective J is maximized to satisfactory precision.

III. ILLUSTRATION AND DISCUSSION

As an example, we consider a pseudomolecular model consisting of four levels $|g\rangle$, $|f\rangle$, $|a\rangle$, and $|b\rangle$ with energies $E_g < E_f < E_a < E_b$, in which $|g\rangle$ and $|f\rangle$ serve as two rovibrational levels in the ground electronic states, and $|a\rangle$ and $|b\rangle$ as two rovibrational levels in the excited electronic states. The control objective J in Eq. (8) is chosen with $O = |f\rangle\langle f|$ and $\rho_0 = |g\rangle\langle g|$ for the population transfer from the initial state $|g\rangle$ to the target state $|f\rangle$. We consider a resonant laser field that couples the two electronic states, so that the direct transitions between $|g\rangle$ and $|f\rangle$ as well as between $|a\rangle$ and $|b\rangle$ can be ignored. As the two levels $|a\rangle$ and $|b\rangle$ are within the spectral range of the pulse, resonant multiphoton transitions between $|g\rangle$ to $|f\rangle$ can occur. Here, we explore whether such multiphoton absorptions can be maximized by optimizing the spectral phase of a single control pulse, which is of fundamental interest for understanding nonlinear optical phenomena [39].

In our simulations, we impose two different types of external constraints on the optimized spectral phases: (1) $h_\ell[\phi(s,\cdot)] = \mathcal{E}(s,t_\ell) = C_\ell$, $\ell = 1,\ldots,(M-1)$, at distinct times $t_1,\ldots,t_{M-1}$, and (2) $h_M[\phi(s,\cdot)] = \int_0^\infty \phi(s,\omega)d\omega = C_M$, where $C_1,\ldots,C_M$ are constants. The coefficients $c_1(s,\omega),\ldots,c_M(s,\omega)$ can be obtained by the functional derivatives $\delta h_1/\delta\phi(s,\omega),\ldots,\delta h_M/\delta\phi(s,\omega)$. Moreover, the spectral phase is further modified by a normalized Gaussian spectral filter $S(\omega'-\omega) = \exp[-4\ln 2(\omega'-\omega)^2/\sigma^2]$ of a bandwidth $\sigma = 80\,\mathrm{cm}^{-1}$. The initial laser field $\mathcal{E}(0,t)$ is taken to be an experimentally accessible Gaussian transform limited (TL) pulse with the peak electric field strength of $\mathcal{E}_0 = 2.4\times 10^{-3}$ a.u., the center frequency of $\omega_0 = 12\,500\,\mathrm{cm}^{-1}$ (800 nm),

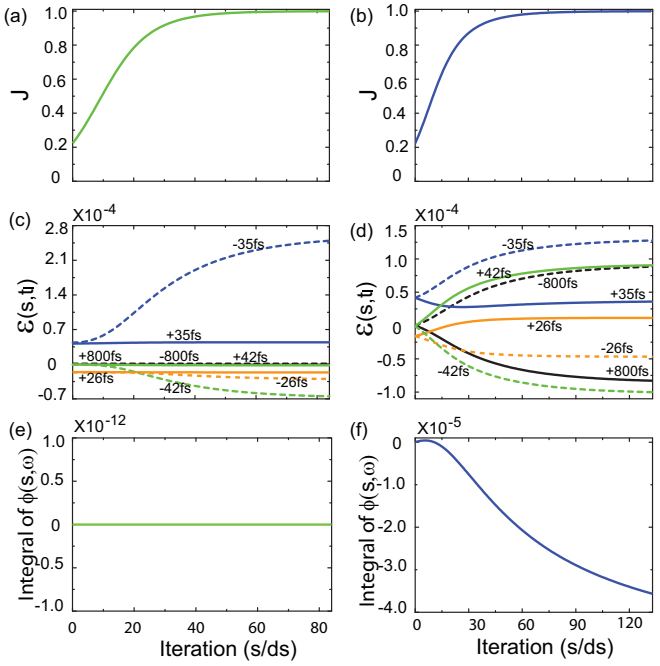

FIG. 1. The spectral-phase-only optimization simulations with (left panels) and without (right panels) the imposed constraints $h_{\ell'}[\phi(s,\cdot)]$, $\ell' = 1,\ldots,6$, as well as the spectral filter. (a),(b) The control objective J corresponding to the population on the target state $|f\rangle$; (c),(d) the values of the optimized laser field at $t = \pm 26, \pm 35, \pm 42$, and ± 800 fs [in (c), the black line of 800 fs overlaps the dashed black line of -800 fs]; and (e),(f) the integral of the optimized spectral phase as a function of the number of iterations (s/ds). The optimization process is terminated when the objective value J is converged to 0.999.

and the full width at half maximum (FWHM) of 30 fs corresponding to a frequency bandwidth $\Delta\omega \approx 980\,\mathrm{cm}^{-1}$. The frequency domain over a window of $3\,000\,\mathrm{cm}^{-1}$ centered at ω_0 is divided evenly into 512 frequency bands with a resolution $d\omega \approx 5.85\,\mathrm{cm}^{-1}$. These parameters ω_0, $d\omega$, $\Delta\omega$, $\mathcal{E}_0$ are fixed throughout to account for the internal limitations involved in SPOOs.

For comparison, Fig. 1 shows the simulations with (left panels) and without (right panels) external constraints including the spectral filter. The energy difference between the two intermediate states, $\Omega' = E_b - E_a$, is assumed to be the same as that between the initial and target states, $\Omega = E_f - E_g = 480\,\mathrm{cm}^{-1}$. The transition dipole moments are chosen as $\mu_{ij} = \langle i|\mu|j\rangle = 1.0$ a.u. for $i = g,f$ and $j = a,b$. The temporal duration of the optimized pulse is fixed at $T = 1\,600$ fs, which can be regarded as another internal limitation from simulations. The temporal constraints are imposed simultaneously on the control field at three intermediate times $t = +26, +35, +42$ and two terminal times $t = \pm 800$ fs. As can be seen in Figs. 1(a) and 1(b), the resonant multiphoton transition probability in the both cases can be monotonically increased to the predetermined value of 99.9% as the dummy variable s increases. Note that the control objective J in the present simulations has almost reached the global extremum of 100%, although strongly demanding and competing constraints may result in the local extrema [35,40].

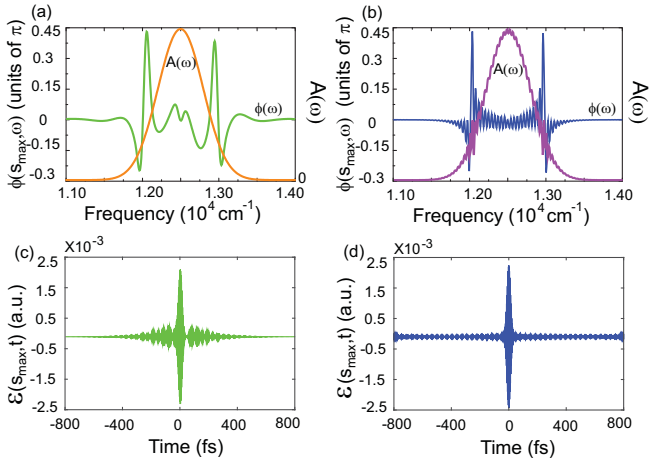

FIG. 2. (a),(b) The final optimized spectral phase as well as the final spectral amplitude, and (c),(d) the corresponding temporal electric field with (left panels) and without (right panels) the imposed temporal and spectral constraints as well as the spectral filter.

The values of the constrained control field in Fig. 1(c) at the five specified times, as expected, are fixed as the initial pulses, while the field at $t = -26, -35, -42$, starting with the same values as those at $t = +26, +35, +42$, undergoes large changes during iterations. The integral of the constrained spectral phase in Fig. 1(e) is fixed throughout the optimization. None of these special features appeared in the unconstrained field; cf. Figs. 1(d) and 1(f).

Figure 2 displays the final optimized spectral phases, the final spectral amplitudes, and the corresponding temporal fields used in Fig. 1. The both constrained spectral phases are modified at three fundamental frequencies around ω_0 and $\omega_0 + \Omega$ for constructing quantum interferences, which lead to the enhancement of population transfer to the target state [39], as shown in Fig. 3. The effect of the involved constraints on the optimized fields can be found in Fig. 2, in which

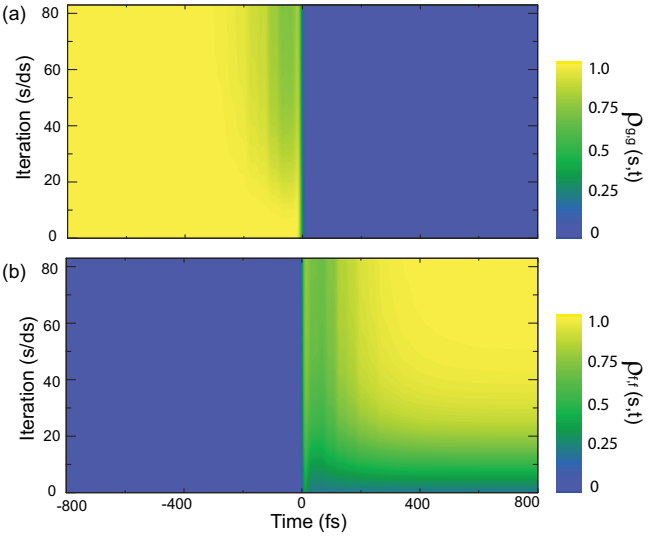

FIG. 3. The population evolution of (a) the initial state $|g\rangle$ and (b) the target state $|f\rangle$ as a function of the number of iterations (s/ds) with constrained spectral-phase-only optimization.

the shape of the constrained spectral phase in Fig. 2(a) looks much smoother than the unconstrained one in Fig. 2(b). The optimized spectral phases will determine the time evolution of the optimized pulses, which are prolonged as compared with the initial TL pulse. The spectral filter $S(\omega' - \omega)$ combined with the two terminal constraints $\mathcal{E}(\pm T/2) = 0$ ensures that the optimized laser field is smoothly turned on and off going from $-T/2$ to $T/2$, as shown in Fig. 2(b). Without the filter function and the two terminal constraints, however, the control field in Fig. 2(d) rapidly spreads out and is suddenly cut off at $t = \pm T/2$, and thus the time range from $-T/2$ to $T/2$ is not enough to transform a full field by using Eq. (1). As can be seen from Fig. 2(b), the spectral amplitude $A(\omega)$ of the final optimized pulse is not the same as the initial pulse, indicating that the unconstrained simulation by Eq. (3) fails to perform the SPOO within a fixed time interval. The present method by introducing the frequency filter and the two terminal constraints provides an alternative approach to perform an "exact" SPOO in simulations, which can localize the optimized pulses while keeping the spectral amplitude fixed. In contrast to the almost symmetric unconstrained spectral phase with respect to the center frequency in Fig. 2(b), the constrained spectral phase in Fig. 2(a) is clearly asymmetric, which in turn results in an asymmetric shape of the temporal field in Fig. 2(c). The temporally asymmetric pulse shaping has potential applications for investigating and controlling quantum dynamics, yielding results that cannot be achieved by using temporally symmetric pulses [41,42].

We also applied the method with different values of Ω and Ω' as well as with various sets of constraints including the temporal duration of T and the filter function. In all cases, the method retained the ability to incorporate multiple constraints on the optimized control field while maintaining monotonic convergence. Note that the application of the method is not limited to the SPOO and the constraints used in the present simulations. To this end, the method may be adopted for multiple constraint spectral-amplitude-only optimization (SAOO) by fixing the spectral phase and imposing spectral amplitude constraints, e.g., $\int_0^\infty A^2(s,\omega)d\omega = \int_0^\infty A^2(0,\omega)d\omega$ for fixing the energy of the optimized pulse unchanged during optimization. The method can also be equally formulated in the time domain for optimizing generalized control fields $\mathcal{E}(t)$ subject to multiple external constraints, e.g., the fluence constraint $\int_{-T/2}^{T/2} \mathcal{E}^2(s,t)dt = \int_{-T/2}^{T/2} \mathcal{E}^2(0,t)dt$.

IV. SUMMARY

We have presented a gradient-based frequency domain quantum optimal control method to optimize time domain ultrafast laser pulses subject to multiple internal limitations as well as external constraints. This optimization method has been successfully employed to perform the SPOO for enhancing the resonant multiphoton transition while taking into account six internal limitations, six external constraints, and one spectral filter. Enhancing such multiphoton transitions may have potential applications in resonant Raman spectroscopy [43,44]. We envision that other spectral phase sensitive quantum coherent phenomena [45–49] can be further optimized within this SPOO framework, and the method can be applied to other control problems in quantum physics including quantum information science [7]. Going beyond simulations, a laboratory-based steepest-ascent algorithm based on Eq. (5) could be implemented, in which flexible external constraints on the optimal field can be rapidly introduced offline with the experimentally measured gradients $\delta J/\delta A(s,\omega)$ and $\delta J/\delta\phi(s,\omega)$ to optimize the laser pulse in an iterative fashion. Since the method makes no assumptions on the nature of the system, the procedure should be amenable to complex quantum systems, especially in the laboratory, for either enhancing or suppressing complex ultrafast photophysical and photochemical phenomena.

ACKNOWLEDGMENTS

This work by C.C.S. and X.X. was partially supported by the Department of Energy (USA) under Grant No. DE-FG02-02ER15344. T.S.H. and H.R. acknowledge partial support by the National Science Foundation (USA) under Grant No. CHE-0718610. C.C.S also acknowledges partial support by the Vice-Chancellor's Postdoctoral Research Fellowship of The University of New South Wales, Australia.

[1] T. Brixner, N. H. Damrauer, P. Niklaus, and G. Gerber, Nature (London) **414**, 57 (2001).
[2] X. H Xie, S. Roither, M. Schöffler, E. Lötstedt, D. Kartashov, L. Zhang, G. G. Paulus, A. Iwasaki, A. Baltuška, K. Yamanouchi, and M. Kitzler, Phys. Rev. X **4**, 021005 (2014).
[3] H. Rabitz, R. de Vivie-Riedle, M. Motzkus, and K. Kompa, Science **288**, 824 (2000).
[4] P. Nuernberger, D. Wolpert, H. Weiss, and G. Gerber, Proc. Natl. Acad. Sci. USA **107**, 10366 (2010).
[5] R. Hildner, D. Brinks, J. B. Nieder, R. J. Cogdell, and N. F. van Hulst, Science **340**, 1448 (2013).
[6] G. D. Fuchs, G. Burkard, P. V. Klimov, and D. D. Awschalom, Nat. Phys. **7**, 789 (2011).
[7] S. J. Glaser, U. Boscain, T. Calarco, C. P. Koch, W. Köckenberger, Ronnie Kosloff, I. Kuprov, B. Luy, S. Schirmer, T. Schulte-Herbrüggen, D. Sugny, and. K. Wilhelm, Eur. Phys. J. D **69**, 279 (2015).
[8] T. Blasi, M. F. Borunda, E. Räsänen, and E. J. Heller, Phys. Rev. B **87**, 241303 (2013).
[9] P. Doria, T. Calarco, and S. Montangero, Phys. Rev. Lett. **106**, 190501 (2011).
[10] T. Choi, S. Debnath, T. A. Manning, C. Figgatt, Z.-X. Gong, L.-M. Duan, and C. Monroe, Phys. Rev. Lett. **112**, 190502 (2014).
[11] J. P. Palao and R. Kosloff, Phys. Rev. Lett. **89**, 188301 (2002).
[12] C. Brif, R. Chakrabarti, and H. Rabitz, New J. Phys. **12**, 075008 (2010).
[13] E. Asplund and T. Klüner, Phys. Rev. Lett. **106**, 140404 (2011).
[14] A. Castro, J. Werschnik, and E. K. U. Gross, Phys. Rev. Lett. **109**, 153603 (2012).

[15] D. J. Egger and F. K. Wilhelm, Phys. Rev. Lett. **112**, 240503 (2014).
[16] C.-C. Shu, M. Edwalds, A. Shabani, T.-S. Ho, and H. Rabitz, Phys. Chem. Chem. Phys. **17**, 18621 (2015).
[17] C.-C. Shu, T. Rozgonyi, L. González, and N. E. Henriksen, J. Chem. Phys. **136**, 174303 (2012).
[18] A. Assion, T. Baumert, M. Bergt, T. Brixner, B. Kiefer, V. Seyfried, M. Strehle, and G. Gerber, Science **282**, 919 (1998).
[19] C. Daniel, J. Full, L. González, C. Lupulescu, J. Manz, A. Merli, S. Vajda, and L. Wöste, Science **299**, 536 (2003).
[20] P. Nuernberger, G. Vogt, T. Brixner, and G. Gerber, Phys. Chem. Chem. Phys. **9**, 2470 (2007).
[21] D. Cardoza, M. Baertschy, and T. Weinacht, Chem. Phys. Lett. **411**, 311 (2005).
[22] J. Roslund and H. Rabitz, Phys. Rev. Lett. **112**, 143001 (2014).
[23] A. M. Weiner, Rev. Sci. Instrum. **71**, 1929 (2000).
[24] A. M. Weiner, Opt. Commun. **284**, 3669 (2011).
[25] J. Werschnik and E. K. U. Gross, J. Phys. B **40**, R175 (2007).
[26] C. Gollub, M. Kowalewski, and R. de Vivie-Riedle, Phys. Rev. Lett. **101**, 073002 (2008).
[27] M. Lapert, R. Tehini, G. Turinici, and D. Sugny, Phys. Rev. A **79**, 063411 (2009).
[28] P. von den Hoff, S. Thallmair, M. Kowalewski, R. Siemering, and R. de Vivie-Riedle, Phys. Chem. Chem. Phys. **14**, 14460 (2012).
[29] J. P. Palao, D. M. Reich, and C. P. Koch, Phys. Rev. A **88**, 053409 (2013).
[30] Daniel M. Reich, José, P. Palao, and C. P. Koch, J. Mod. Opt. **61**, 822 (2014).
[31] D. Sugny, S. Vranckx, M. Ndong, N. Vaeck, O. Atabek, and M. Desouter-Lecomte, Phys. Rev. A **90**, 053404 (2014).
[32] A. K. Tiwari and N. E. Henriksen, J. Chem. Phys. **141**, 204301 (2014).
[33] C.-C. Shu and N. E. Henriksen, J. Chem. Phys. **136**, 044303 (2012).
[34] M. Shapiro and P. Brumer, *Quantum Control of Molecular Processes* (Wiley, Weinheim, Germany, 2012).
[35] K. W. Moore and H. Rabitz, J. Chem. Phys. **137**, 134113 (2012).
[36] A. Rothman, T.-S. Ho, and H. Rabitz, Phys. Rev. A **72**, 023416 (2005).
[37] T.-S. Ho and H. Rabitz, J. Chem. Phys. **104**, 2584 (1996).
[38] J. Roslund and H. Rabitz, Phys. Rev. A **79**, 053417 (2009).
[39] N. Dudovich, B. Dayan, S. M. Gallagher Faeder, and Y. Silberberg, Phys. Rev. Lett. **86**, 47 (2001).
[40] G. Riviello, K. M. Tibbetts, C. Brif, R. X. Long, R. B. Wu, T.-S. Ho, and H. Rabitz, Phys. Rev. A **91**, 043401 (2015).
[41] W. P. Leemans, P. Catravas, E. Esarey, C. G. R. Geddes, C. Toth, R. Trines, C. B. Schroeder, B. A. Shadwick, J. van Tilborg, and J. Faure, Phys. Rev. Lett. **89**, 174802 (2002).
[42] J. Hernandez-Rueda, N. Götte, J. Siegel, M. Soccio, B. Zielinski, C. Sarpe, M. Wollenhaupt, T. A. Ezquerra, T. Baumert, and J. Solis, Appl. Mater. Interfaces **7**, 6613 (2015).
[43] C. Neumann, S. Reichardt, P. Venezuela, M. Drögeler, L. Banszerus, M. Schmitz, K. Watanabe, T. Taniguchi, F. Mauri, B. Beschoten, S. V. Rotkin, and C. Stampfer, Nat. Commun. **6**, 8429 (2015).
[44] G. Wang, M. M. Glazov, C. Robert, T. Amand, X. Marie, and B. Urbaszek, Phys. Rev. Lett. **115**, 117401 (2015).
[45] M. C. Stowe, A. Péer, and J. Ye, Phys. Rev. Lett. **100**, 203001 (2008).
[46] L. A. Pachón, L. Yu, and P. Brumer, Faraday Discuss. **163**, 485 (2013).
[47] D. Brinksa, M. Castro-Lopeza, R. Hildnera, and N. F. van Hulst, Proc. Natl. Acad. Sci. USA **110**, 18386 (2013).
[48] I. Barmes, S. Witte, and K. S. E. Eikema, Nat. Photon. **7**, 38 (2012).
[49] E. Wells, C. E. Rallis, M. Zohrabi, R. Siemering, B. Jochim, P. R. Andrews, U. Ablikim, B. Gaire, S. De, K. D. Carnes, B. Bergues, R. de Vivie-Riedle, M. F. Kling, and I. Ben-Itzhak, Nat. Commun. **4**, 2895 (2013).